

effective, overall characteristics. The tendency for k_0 , F , and n to become independent of the heating rate on increasing the latter may be explained on the same general basis.

LITERATURE CITED

1. V. D. Moiseev, N. G. Avetisyan, A. G. Chernova, and A. A. Atruskevich, *Plast. Massy*, 12, No. 3 (1971).
2. E. Calvet and H. Prat, (editors), *Recent Progress in Microcalorimetry*, Pergamon (1963).
3. N. I. Basov, Yu. V. Kazankov, A. I. Leonov, V. A. Lyubortovich, and V. A. Mironov, *Izv. Vyssh. Uchebn. Zaved., Khim. Khim. Tekhnol.*, 12, No. 11 (1969).

A 2-MW HYDROGEN PLASMOTRON

R. Ya. Zakharkin, A. V. Pustogarov,
and Yu. V. Kurochkin

UDC 533.9.07

An end-plane type plasmotron permitting generation of high-pressure high-temperature hydrogen flows with mean mass temperature from 2000 to 5000°K is considered.

The development of a number of projects in the fields of plasmochemistry and metallurgy requires the use of low-temperature hydrogen-plasma generators at a power level of 1-10 MW at operating times up to 100 h, with high efficiency with respect to transformation of electrical energy into flow thermal energy. The specifics of some technological processes demand important additional requirements in the generator: high hydrogen purity (absence of electrode material impurities), ability to vary temperature, flow rate, and pressure over wide ranges, reproducibility of parameters from operation to operation, and minimal parameter pulsation during operation.

Plasmotrons operating with air, nitrogen, and inert gases have been studied thoroughly, and their power level has been increased to 50 MW [1]. However, conversion of such plasmotrons to operation with hydrogen produces significant difficulties connected with the increase in energy liberation in the electrode regions [2] and decrease in stability of the arc discharge. Of existing hydrogen plasmotrons, those with power greater than 1 MW are of practical interest (Table 1).

The gas turbulence plasmotron of [3] has high efficiency and is capable of continuous operation for hundreds of hours. However, use of graphite electrode coatings leads to enrichment of the hydrogen plasma by carbon. In the operation of the coaxial hydrogen plasmotron of [2] the significant erosion of the central electrode limits operating time even with use of porous tungsten filling. Improvements of this method led to creation of plasmotrons with electrode gas curtains at places of arc contact, which allows generation of a flow of hydrogen-containing working plasma at pressures up to 50 atm. The end-plane type plasmotron allows combination of the advantages of the gas turbulence system (high efficiency) and the coaxial system (high pressure).

The present study will offer results of an experimental investigation of an end-plane type plasmotron with a power level of 2 MW.

1. Plasmotron Operation

The plasmotron construction consists of a thermocathode formed of lanthanum-coated tungsten ($V_L = 10$, $d_C = 7-10$ mm, $l_C = 70-120$ mm), soldered to a water-cooled copper nozzle, intermediate electrical insulation, and an anode ($d_a = 20, 40, \text{ and } 74$ mm) with a solenoid mounted on it [4]. Figure 1 presents the volt-ampere characteristics and the mean mass hydrogen temperature of the plasmotron. Thermal efficiency is limited mainly by anode losses which increase linearly with current [5]. With an increase in the arc chamber diameter

Translated from *Inzhenerno-Fizicheskii Zhurnal*, Vol. 29, No. 6, pp. 1084-1090, December, 1975. Original article submitted December 25, 1974.

This material is protected by copyright registered in the name of Plenum Publishing Corporation, 227 West 17th Street, New York, N.Y. 10011. No part of this publication may be reproduced, stored in a retrieval system, or transmitted, in any form or by any means, electronic, mechanical, photocopying, microfilming, recording or otherwise, without written permission of the publisher. A copy of this article is available from the publisher for \$7.50.

TABLE 1. Hydrogen Plasmotron Parameters

Reference	Anode diameter, d_a , mm	Cathode diameter d_c , mm	Arc current I, kA	Arc voltage U, kV	Plasmotron power N, MW
[3]	105	300-500	1,15	7,0	8,2
[2]	170	180	4-7	0,2-0,5	2,4
Present study	20	7-10	0,1-1,2	0,2-0,7	0,04-0,4
	40		0,4-1,4	0,4-1,4	0,3-1,2
	74		0,4-1,4	0,8-2,0	0,5-2,0

Reference	Hydrogen flow rate G, g/sec	Mean mass temperature T_{mm} , 10^3 °K	Pressure P, atm	External magnetic field H, kG	Thermal efficiency η	Operating time τ , h
[3]	—	—	1	—	0,75	200
[2]	3-7	up to 4,5	6	up to 6,0	0,3	—
Present study	1-5	2 ÷ 5	1-25	0,6-1,0	0,7-0,8	1-10
	5-20		1-10		0,7-0,85	
	10-40		1-8		0,7-0,8	

from 20 to 74 mm the arc voltage at $I=800$ A increases from 300 to 1400 V, which produces an increase in flow power despite increased thermal losses [4]. Pressure increases in the discharge chamber leads to increased anode losses due to increased radiation from the arc column and convective losses from the closed gas flow. As for inert gases [6], the arc voltage is proportional to pressure to the ~ 0.5 power. Thus with increase in pressure, efficiency decreases, but because of the significant increase in discharge voltage the heat injected into the gas increases and hydrogen temperature increases. The effect of gas flow rate on voltage, efficiency, and anode thermal losses, according to [5], is insignificant.

It is interesting to compare the characteristics of this plasmotron operating with various working substances. Figure 2 shows plasmotron parameters ($d_a = 40$ mm, $P = 4$ atm, $G = 10$ g/sec) with use of Ar, He, and H_2 . Arc voltages at $I = 800$ A for Ar, He, and H_2 are in the ratio 1:4.3:13.7, while specific enthalpy for Ar is 0.9; He, 13.5; H_2 , 75 kJ/g. Thermal losses at the cathode are negligibly small for He and H_2 , and comprise 5% of the anode losses for Ar. Increase in external magnetic field intensity for Ar leads to decrease in anode losses, and, consequently, to increase in mean mass temperature and efficiency [7]. In the He and H_2 atmospheres increase in magnetic field intensity increases the convective component of anode heat loss, and efficiency and mean mass gas temperature are decreased.

A generalization of the volt-ampere characteristics over the basic parameter range studied for operation with Ar, He, and H_2 allowed us to obtain the dimensionless voltage drop as a function of the Kutateladze and Euler criteria, inasmuch as other criteria have an insignificant effect on the volt-ampere characteristic:

$$U d_a \sigma_0 / I = 0.069 (I^2 / G d_a \sigma_0 h_0)^{-0.54} (\rho_0 P d_a^4 / G^2)^{0.187},$$

where U, V; d_a , cm; σ_0 , mho/cm; I, A; G, g/sec; h_0 , J/g; ρ_0 , g/cm³.

Experimental point scattering comprises $\pm 30\%$, reducing to $\pm 10\%$ for each individual gas. The thermo-physical parameters were determined with the method of [8].

According to the above formula, by increasing anode diameter to 200 mm, pressure to 20 atm, and hydrogen flow rate to 100 g/sec a power level of 5 MW may be attained at a current of 1000 A, with 7.5 MW at 2000 A.

2. Electrode Erosion Stability

It is well known that plasmotron operating time is limited by the time required for electrode failure [9]. Tests have revealed a significant dependence of thermocathode erosion on geometry. Decrease in cathode diameter from 10 to 7 mm increases erosion rate \bar{G} by an order (Table 2). Minimum \bar{G} values in operation with hydrogen are observed in the current range $I = 200-750$ A. With further increase in I erosion increases and may attain a "critical" value characterized by removal of droplets of electrode material.

At atmospheric pressure for a thermocathode with $d_c = 10$ mm and $l_c = 80-100$ mm the "critical" regime sets in for H_2 at $I = 900$ A, for Ar at $I = 2200$ A, and for He at $I = 3000$ A. Pressure increase from 1 to 10 atm produces increase in erosion for He by an order, and for H_2 by two orders.

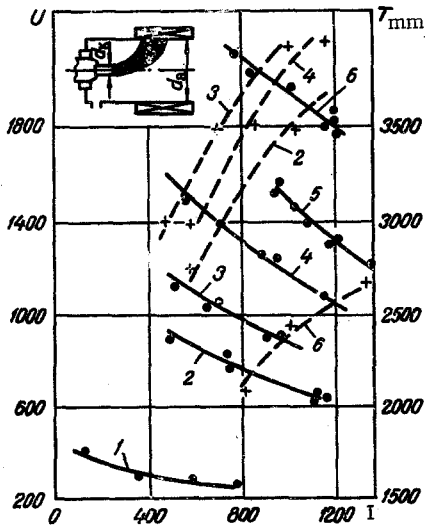


Fig. 1

Fig. 1. Plasmotron parameters: (solid lines, volt-ampere characteristic; dashed lines, T_{mm}): 1) $d_a = 20$, $P = 1$, $G = 3$; 2) 40; 4; 10; 3) 40; 6; 10; 4) 74; 3; 16; 5) 74; 4; 20; 6) 74, 8, 40. U, V; I, A; T_{mm} , °K; d_a , mm; P, atm; G, g/sec.

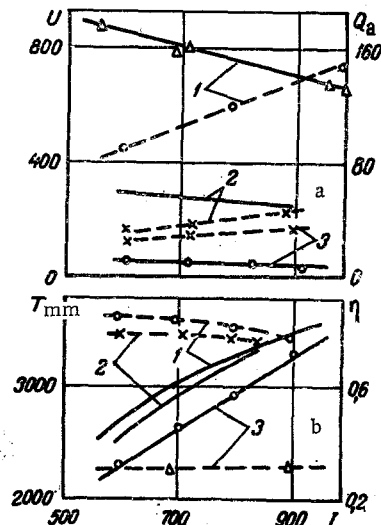


Fig. 2

Fig. 2. Plasmotron parameters for various working gases: ($P = 4$ atm, $G = 10$ g/sec, $d_a = 40$ mm); a) solid line, volt-ampere characteristic; dashed line; Q_a ; b) solid line, T_{mm} ; dashed line, η . 1) H_2 , 2) He, 3) Ar; U, V; I, A; Q_a , kW; T_{mm} , °K.

Comparison of cathode efficiency in operation with different substances indicates increased erosion upon transition from He to Ar and H_2 . Thus, for example, at $I = 600$ A, $P = 1$ atm, $d_c = 10$ mm, $l_c = 80-100$ mm, $\bar{G} = 2 \cdot 10^{-8}$ g/C for He, $\bar{G} = 6 \cdot 10^{-8}$ g/C for Ar, and $\bar{G} = 10^{-7}$ g/C for H_2 .

This fact, as is confirmed by a high-speed moving-picture and the state of the cathode surface after operation, is explained by the character of the arc contact, which in the case of He is diffuse, for Ar, diffuse with a clearly defined central core, and for H_2 , contracted. Thus, in operation with H_2 , any mechanism causing motion of the arc contact over the "cold" cathode surface (nonuniform draft, external magnetic field, electrode parameter pulsation, etc.) will lead to significant cathode erosion.

The state of the anode surface ($d_a = 40$ and 74 mm) operating in the complex for more than 10 h indicates the absence of noticeable erosion. Thus, for 12-min tests in a hydrogen atmosphere ($d_a = 20$ mm, $I = 600$ A, $P = 1$ atm) the erosion was $1.5 \cdot 10^{-8}$ g/C. This indicates that operating time of an end-plane type hydrogen plasmotron is limited by cathode effectiveness.

3. Estimate of Hydrogen-Plasmotron Operating Time.

The study performed permits analysis of possibilities for increasing hydrogen-plasmotron operating time to, for example, 100 h. Experiments show that decrease in the thermocathode length from 100 to 80-70 mm does not lead to change in the plasmotron output characteristics. If it is assumed that tungsten thermocathode erosion is constant in lengthy operation, then the greatest erosion rate at which the thermocathode will be expended by an admissible amount over a 100-h operating time will be $\bar{G} = 3 \cdot 10^{-7}$ g/C.

An experimental study of thermocathode erosion stability as a function of current and pressure allowed determination of the permissible erosion region (below curve 1, Fig. 3). Increase in pressure in the arc chamber while maintaining the admissible erosion rate requires reduction in the discharge current. However, for a fixed arc-chamber diameter there exists a region of operating conditions (curve 2, Fig. 3), limited below by the minimum current value required for stable arc burning, which is dependent on the external ballast resistance R_b (in our case $R_b = 2\Omega$). Thus, 100 h of operation at $d_a = 74$ mm may be realized in the current range 500-700 A at pressures of 1-1.7 atm with maximum power of 700 kW.

Increase in plasmotron power is possible by increase in anode diameter, since according to Fig. 3 the minimum current value of 700 A corresponds to $d_a = 100$ mm. In this case, without leaving the admissible operation region the plasmotron power at atmospheric pressure may be 1 MW, which heats 20 g/sec of hydrogen to $T_{mm} = 3000^\circ\text{K}$.

TABLE 2. Effect of Various Parameters on Thermocathode Erosion

Arc current I, A	Pressure P, atm	Cathode diameter d_c , mm	Cathode length l_c , mm	Anode diameter d_a , mm	Gas type	Gas flow rate G, g/sec	Test time τ , min	Cathode erosion G, g/C
1000	4,0	10	110	74	H ₂	20	2	$2,7 \cdot 10^{-5}$
1000	4,0	9	110	74	H ₂	20	2	$1,0 \cdot 10^{-4}$
1000	4,0	8	110	74	H ₂	20	2	$1,7 \cdot 10^{-4}$
1000	4,0	7	110	74	H ₂	20	2	$2,6 \cdot 10^{-4}$
220	4,0	10	80	20	H ₂	5	4	$4,2 \cdot 10^{-6}$
300	4,0	10	80	20	H ₂	5	4	$3,8 \cdot 10^{-6}$
510	4,0	10	80	20	H ₂	5	4	$1,0 \cdot 10^{-5}$
700	4,0	10	80	20	H ₂	5	4	$1,1 \cdot 10^{-5}$
950	4,0	10	80	20	H ₂	5	4	$6,2 \cdot 10^{-4}$
150	1,0	10	80	74	He	2,0	10	$5 \cdot 10^{-8}$
1200	1,0	10	80	74	He	20	10	$3 \cdot 10^{-8}$
2400	1,0	10	80	74	He	20	10	$1 \cdot 10^{-7}$
610	1	10	80	20	H ₂	5	12	$1,0 \cdot 10^{-7}$
350	1	10	80	20	H ₂	5	4	$1,7 \cdot 10^{-7}$
350	4,0	10	80	20	H ₂	5	4	$3,8 \cdot 10^{-6}$
350	7,0	10	80	20	H ₂	5	4	$1,9 \cdot 10^{-5}$
350	13,0	10	80	20	H ₂	5	4	$4,05 \cdot 10^{-5}$
1000	1,0	10	10	74	He	20	10	$5,0 \cdot 10^{-8}$
1000	10	10	10	74	He	20	10	$3,0 \cdot 10^{-7}$

Further increase in power by changes in current, pressure, and discharge chamber dimensions will be accompanied by significant reduction in operating time.

4. Methods for Increasing Plasmotron Power

Further increase in plasmotron power while preserving the operating time may be achieved by increase of either current or voltage. The first may be achieved by uniformly distributing the total current over several cathodes (Fig. 4), or by protection of the cathode by inert gas.

In the combined plasmotron (Fig. 4a) the auxiliary plasmotron 1 (power ~ 100 kW) ensures heating of the main thermocathodes 2 and smooth ignition of the main discharge 3 between cathodes 2 and anode 4. The main and auxiliary anodes have solenoids for curving the arcs. Another method of dividing current is the multiarc plasmotron (Fig. 4b). The arc discharges burn between cathodes 1, installed in a cooled body 2, and anodes 3. Discharge movement over the anode is accomplished by drive mechanism 5. Gas discharge 6, 7 is conducted before each discharge zone.

Studies performed have shown that an inert gas (Ar, He) draft into a cylindrical slit gap at the cathode base can reduce the erosion rate to $3 \cdot 10^{-7}$ g/C at $I=1000-1100$ A and $P = 3-4$ atm. However, in some cases this proves inapplicable from the economic standpoint.

A second, more promising approach is increase in the volt-ampere ratio by use of an increased arc length, i.e., the higher power is attained by a higher voltage value with limited discharge current value, ensuring long electrode lifetime.

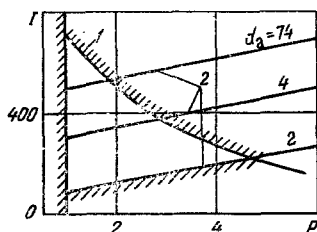


Fig. 3.

Fig. 3. Permissible operation region. I, A, P; atm; d_a , cm.

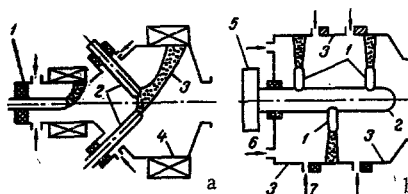


Fig. 4

Fig. 4. Diagrams of plasmotrons with current division over several cathodes.

We note that in this case it is expedient to have a rising volt-ampere characteristic, allowing operation in a rheostatless mode, i.e., with an electrical efficiency close to unity. However, obtaining a rising volt-ampere characteristic in the case of hydrogen is difficult. Calculations performed for a flowless arc column in a cylindrical channel show that because of the linear dependence of electrical conductivity σ on thermal conductivity function S ($S = \int_0^T \kappa dT$) in the temperature range up to 10^5 °K it is impossible to obtain a rising volt-ampere characteristic, in contrast to other gases (Ar, He, N₂). This is because in other gases the possibility of ionization with temperature increase retards the growth of σ , the latter explaining the rising volt-ampere characteristic. The results of [10] show that even for a stabilizing channel diameter of $d = 1.5$ mm, current of 400 A, gas temperature on axis $T_0 = 25 \cdot 10^3$ °K, and electric field intensity $E = 100$ V/cm, the volt-ampere characteristic does not move to the ascending branch.

Because of the difficulty of achieving a rising volt-ampere characteristic in hydrogen plasmotrons, special electrical power supplies with a sharply falling characteristic are required. For sources with good regulation stable operation of end-plane hydrogen plasmotrons requires an active (ballast) resistance in which 30-40% of the required power is dissipated.

Of the methods of increasing power considered here, the most promising appears to be the one related to distribution of current over several cathodes, each of which will then operate in the permissible region. In this case power increase will be practically proportional to the number of thermocathodes, while operating time will be preserved at the 100-h level.

NOTATION

d , diameter; l , cathode length; I , arc current; U , arc voltage; G , gas flow rate; T , temperature; H , magnetic field intensity; P , pressure; η , thermal efficiency; τ , operating time; \bar{G} , electrode erosion rate; ΔU_a , current equivalent of anode heat losses; N , thermal power of jet; Q , thermal losses; κ , thermal conductivity; σ , electrical conductivity; ρ , density; h , enthalpy. Indices: a , anode; c , cathode; m , mean mass; o , arc boundary.

LITERATURE CITED

1. R. T. Smith and I. L. Folck, AFFDL-TR-69-6 (1969).
2. A. S. Koroteev, M. A. Lomovtsev, and P. P. Mayakin, in: Plasma Jet and High-Power Arc Generators [in Russian], Nauka, Moscow (1973).
3. H. Gladisch, Petroleum Refiner, 41, No. 6 (1962).
4. R. Ya. Zakharkin, A. V. Pustogarov, B. S. Gavryushenko, and Yu. V. Kurochkin, in: Proceedings of the Sixth All-Union Conference on Low-Temperature Plasma Generators [in Russian], Frunze (1974).
5. R. Ya. Zakharkin and A. V. Pustogarov, Inzh.-Fiz. Zh., 23, No. 1 (1972).
6. R. Ya. Zakharkin, A. N. Kolesnichenko, É. I. Molodykh, and A. V. Pustogarov, in: Proceedings of the Fourth All-Union Conference on Physics and Low-Temperature Plasma Generators [in Russian], Alma-Ata (1970).
7. R. Ya. Zakharkin, A. V. Pustogarov, A. N. Kolesnichenko, and É. I. Molodikh, Inzh.-Fiz. Zh., 21, No. 5 (1971).
8. R. Ya. Zakharkin, A. V. Pustogarov, and Yu. V. Kurochkin, in: Proceedings of the Fifth All-Union Conference on Low-Temperature Plasma Generators [in Russian], Vol. 1, Novosibirsk (1972).
9. M. F. Zhukov, Teplofiz. Vys. Temp., 10, No. 6 (1972).
10. R. R. John, AIAA J., 1, No. 11 (1963).